**Supplemental Information**

**Supplemental Figures**

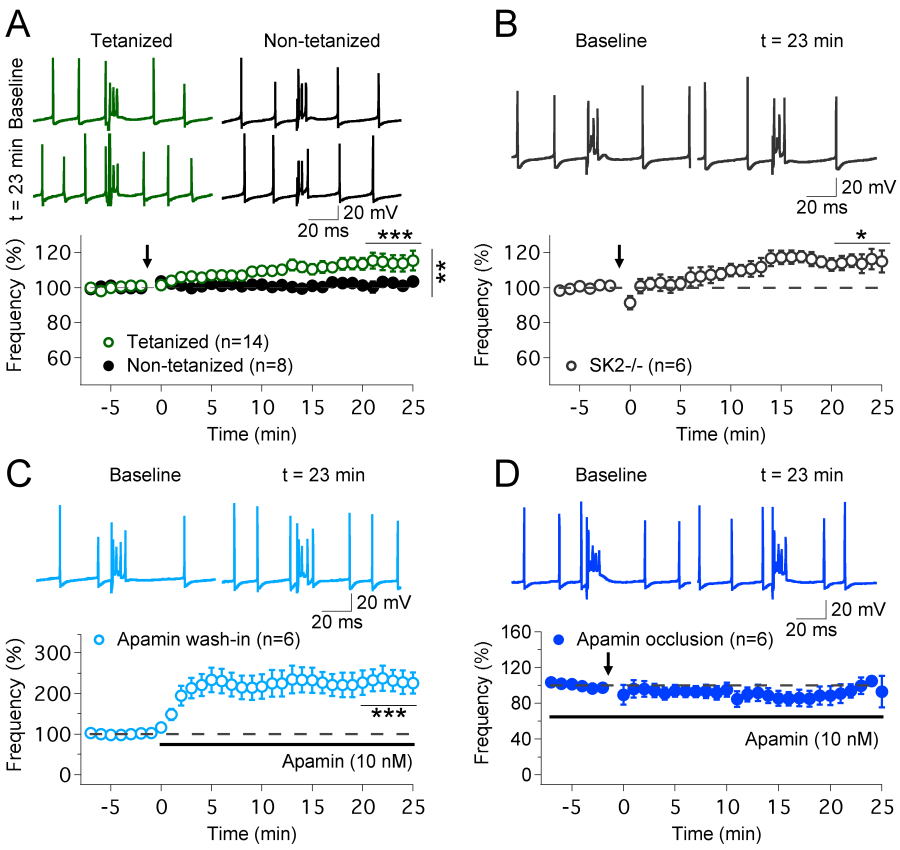


**Figure S1, related to Fig. 2. Pause plasticity is accompanied by an increase in spike frequency**

The spike frequency changes summarized here were obtained from the same recordings that are shown in Fig. 2B-E. In these recordings, we determined the spike frequency rather than the spike count. While the spike count is an appropriate measure for the analysis of excitability as tested by short current pulses (see Fig. 1), the spike frequency is a better measure for assessing effects on prolonged tonic firing (see Fig. 2A). (**A**) IP protocol, tetanized group: 114.1 ± 3.6%, n=14; p=0.0007. Control group: 101.0 ± 2.2%; n=8; p=0.5257. The spike frequency changes observed in the two groups were significantly different from

each other (p=0.0095; Mann-Whitney U-test). (**B**) SK2$^{-/-}$ Purkinje cells: 114.8 ± 3.8%; n=6; p=0.0205. This outcome seems at odds with the absence of changes in spike count in SK2$^{-/-}$ Purkinje cells reported in Fig. 1 A+B. A number of factors might contribute to this discrepancy. The experimental conditions are very different between these recordings, because the experiments illustrated in Fig. 2 and Fig. S1 were optimized for pause measures. In these recordings, it took ≥ 10-15 min longer to stabilize pause and frequency parameters before recording a baseline, possibly causing a partial 'wash-out' effect. For this reason, we strengthened tetanization by increasing its duration (7-8s, instead of 3s as used for the recordings shown in Fig. 1) and by injecting higher amplitude currents (500-700pA vs 100-200pA), which may have resulted in the recruitment of residual IP components in SK2$^{-/-}$ Purkinje cells. The observation that pause plasticity is blocked under these conditions in SK2$^{-/-}$ mice (Fig. 2C), but the increase in spike frequency it unaffected (Fig. S1B) demonstrates that the presence of SK2 channels is essential for pause plasticity, but that other voltage- or calcium-activated ion channels may play a role in the increase in spike frequency that is seen in intrinsic plasticity as assessed here. (**C**) Wash-in of apamin (10nM): 229.4 ± 28.8%; n=6; p=0.0025. (**D**) Apamin (10nM) occlusion: 89.5 ± 9.9%; n=6; p=0.3522. Values are shown as mean ± SEM. *p<0.05; **p<0.01; ***p<0.001.

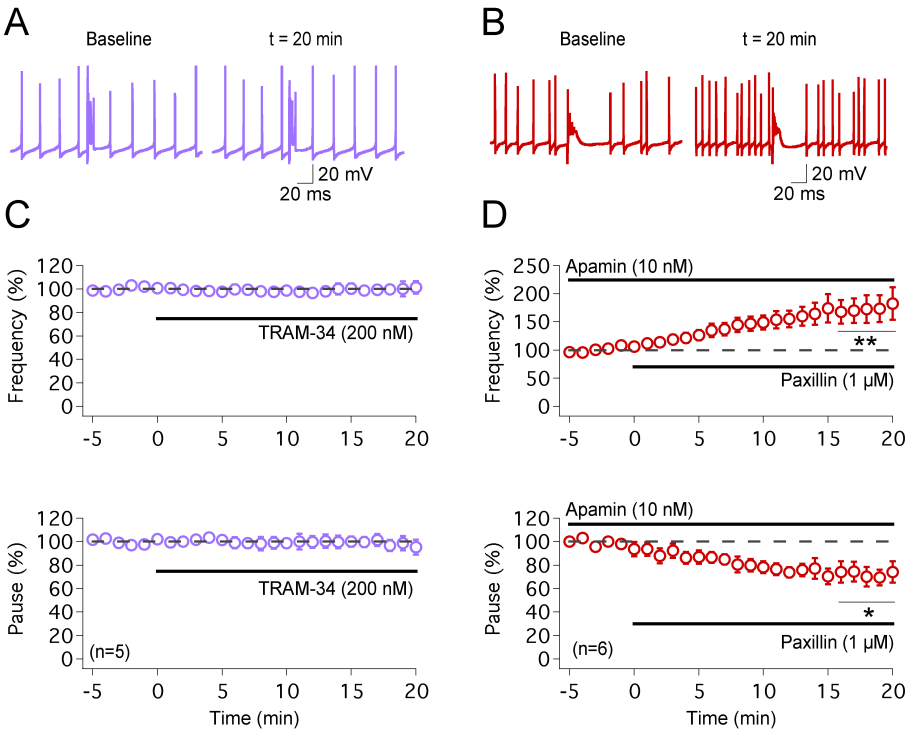


**Figure S2, related to Fig. 2. Calcium-activated BK-type, but not IK -type, $K^+$ channels contribute to the spike pauses and the regulation of spike firing**

The apamin wash-in experiments shown in Fig. 2D demonstrate that SK2 conductances contribute to the spike pause. However, we did not find significantly shortened baseline pause durations in $SK2^{-/-}$ mice, or in the apamin occlusion experiments (WT controls: 42.7 ± 5.9ms; n=14; $SK2^{-/-}$: 38.8 ± 3.4ms; n=6; p=0.7415; apamin occlusion: 32.0 ± 3.5ms; n=6; p=0.4579). To examine whether other types of calcium-activated $K^+$ channels may contribute to the pauses, we tested for effects of the IK channel inhibitor TRAM-34 and the BK channel inhibitor paxillin. (**A**) Wash-in of TRAM-34 (200nM) neither affected the spike frequency nor the pause duration (n=5). (**B**) We have previously shown that BK channel

blockade increases the spike count (Belmeguenai et al., *J. Neurosci*. 30, 2010). Here, we therefore went one step further and specifically asked whether BK channel blockade affects the spike frequency and/or pause duration when SK channels are blocked in the presence of apamin (10nM) in the bath. Under these conditions, paxillin (1μM) wash-in enhanced the spike frequency and shortened the pause duration (n=6). Thus, BK channels, but not IK channels, complement SK2 channels in the control of spike activity and pause length, and BK channels may enable Purkinje cells to maintain spike pauses when SK2 channel activity is blocked. Note, however, that our findings shown in Fig. 2C-E demonstrate that pause plasticity can be explained by SK2 channel downregulation alone, without an explicit need for additional mechanisms. In contrast, spike frequency plasticity may or may not involve conductances other than SK2 (see Fig. S1B) depending on the recording conditions. In a previous study we did not find evidence for an involvement of BK channels in intrinsic plasticity (spike count; Belmeguenai et al., *J. Neurosci*. 30, 2010). Values are shown as mean ± SEM. *p<0.05; **p<0.001.

## Supplemental Experimental Procedures

### Data analysis

The complex spike pause was defined as the time between the complex spike onset (fast spike component) and the next subsequent simple spike (for a discussion of the complex spike waveform, see Schmolesky et al., 2002). This definition was chosen, because of previous reports showing that the low-amplitude spikelets following the first spike component typically have an axonal propagation probability ≤ 50% (Khaliq and Raman, 2005; Monsivais et al., 2005). Thus the silent pause period that is most relevant for axonal propagation and for the communication with the target cells in the cerebellar nuclei is the

period between the first spike component of the complex spike and the next following simple spike. The spike frequency was calculated based on the 8 ISIs preceding the complex spike (Fig. S1). Data points were averaged over the course of one minute of recordings. Baseline values were calculated from the last 5 minutes preceding any stimulus protocol or pharmacological manipulation. Post-induction effects were measured during the last 5-6 minutes of recording. For the analysis of data shown in Fig. 3H, every pause was normalized to the average ISI measured from the 8 ISIs preceding the same complex spike (pause/ISI). For the analysis of the distribution of ISIs (Fig. 3A), spikes were monitored during a 200ms-time window following the complex spike. The ISI values were normalized to the median of the ISI taken from a 100ms time window preceding the complex spike during the baseline period in each individual cell. The % fraction (ISI distribution) was calculated for the baseline and post-tetanization period of every cell before plotting the average distribution. Kurtosis was calculated as a measure of "peakedness" for the distribution of each cell before and after tetanization (Fig. 3B; Kurtosis=0 for normal distribution and negative for more 'flat' distributions). To align the peaks to their own median value and compare the tails of the distributions (Fig. 3C) the ISIs were rescaled by normalization to the median ISI of each distribution (individual cells). For Fig. 3E-G, median ISIs were measured from the 8 ISIs preceding the complex spike and averaged over time.

**Supplemental References**

Khaliq, Z.M. & Raman, I.M. (2005). Axonal propagation of simple and complex spikes in cerebellar Purkinje neurons. J.Neurosci. *25*, 454-463.

Monsivais, P., Clark, B.A., Roth, A. & Häusser, M. (2005). Determinants of action potential propagation in cerebellar Purkinje cell axons. J. Neurosci. *25*, 464-472.

Schmolesky, M.T., Weber, J.T., De Zeeuw, C.I. & Hansel, C. (2002). The making of a complex spike: ionic composition and plasticity. Ann. N. Y. Acad. Sci. *978*, 359-390.